

Spontaneous Formation of a Superconducting and Antiferromagnetic Hybrid State in SrFe₂As₂ under High Pressure

K. Kitagawa,^{1,*} N. Katayama,^{1,†} H. Gotou,¹ T. Yagi,¹ K. Ohgushi,^{1,2} T. Matsumoto,¹ Y. Uwatoko,^{1,2} and M. Takigawa^{1,2}

¹*Institute for Solid State Physics, University of Tokyo, Kashiwanoha, Kashiwa, Chiba 277-8581, Japan*

²*JST, TRIP, 5 Sanbancho, Chiyoda, Tokyo 102-0075, Japan*

(Received 21 July 2009; revised manuscript received 3 November 2009; published 15 December 2009)

We report a novel superconducting (SC) and antiferromagnetic (AF) hybrid state in SrFe₂As₂ revealed by ⁷⁵As nuclear magnetic resonance (NMR) experiments on a single crystal under highly hydrostatic pressure up to 7 GPa. The NMR spectra at 5.4 GPa indicate simultaneous development of the SC and AF orders below 30 K. The nuclear spin-lattice relaxation rate in the SC domains shows a substantial residual density of states, suggesting proximity effects due to the spontaneous formation of a nanoscale SC-AF hybrid structure. This entangled behavior is a remarkable example of a self-organized heterogeneous structure in a clean system.

DOI: 10.1103/PhysRevLett.103.257002

PACS numbers: 74.70.Dd, 64.75.Yz, 74.62.Fj, 76.60.-k

Competition between magnetism and superconductivity is ubiquitous in unconventional superconductors such as cuprates and heavy fermions [1], as is the case for iron pnictides [1,2]. Precise determination of the phase diagram, in particular, whether the antiferromagnetic (AF) and the superconducting (SC) phases mutually exclude or coexist, is often hampered by compositional and structural inhomogeneity, which are inevitable when the SC state is induced by carrier doping [3,4].

While this is the case for cuprates, there is another route to the SC state in iron pnictides. SrFe₂As₂ shows a phase transition from the tetragonal paramagnetic (PM) state into the orthorhombic AF state below 200 K at ambient pressure [5,6]. It is reported to become SC not only by chemical substitution [7,8] to change carrier concentration but also by applying sufficiently high pressure to suppress the AF state [9–11]. The pressure-induced SC state provides an opportunity to unravel intrinsic behavior caused by interplay between the AF and SC order unaffected by disorder. This motivated us to perform high-pressure NMR spectroscopy, a powerful tool to examine coexistence of the SC and AF states.

We developed a new type of opposed-anvil pressure cell [12], which enables NMR experiments in quasihydrostatic pressure up to 9.4 GPa by using argon as the pressure transmitting medium [13]. The cell was mounted on a geared double-axis goniometer allowing precise sample alignment within 1°. The single crystals of SrFe₂As₂ were prepared by self-flux method. A small piece (1 × 0.7 × 0.15 mm³) was cut from the sample used in the study at ambient pressure [6]. NMR signals from Sn and Pt foil were used to determine pressures *in situ* [12].

Figure 1 shows the ⁷⁵As-NMR spectra in the PM and AF states at various *P*. The quadrupole interaction splits the resonance of ⁷⁵As nuclei with spin *I* = 3/2 into three lines corresponding to the transitions *I*_z = *m* ↔ *m* − 1 (*m* = ±1/2, 3/2) at the frequencies $f_{\text{res}} = \gamma|\mathbf{H} + \mathbf{H}_{\text{hf}}| + (m - 1/2)\nu + (\text{second-order quadrupole shift})$, where $\gamma =$

7.2902 MHz/T is the gyromagnetic ratio, H_{hf} is the hyperfine field from the Fe spins, and ν is proportional to the electric field gradient along the field direction. In the PM state, H_{hf} is uniquely given and proportional to the external field, $H_{\text{hf}}^{\alpha} = K^{\alpha}H^{\alpha}$, where K^{α} is the Knight shift along the

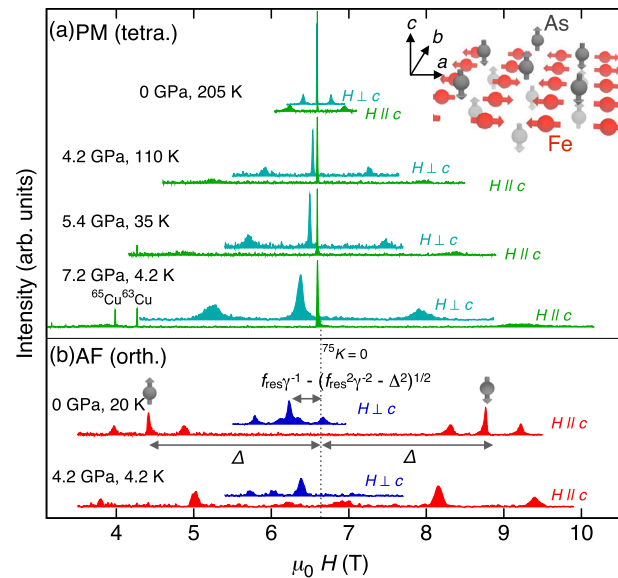


FIG. 1 (color online). ⁷⁵As-NMR spectra of 48.31 MHz at various *P*. (a) The spectra in the PM tetragonal normal state (slightly above *T_N* or *T_C*) for *H* || *c* (green) and *H* ⊥ *c* (sky blue). Although the central line for *H* ⊥ *c* becomes broader at higher *P* due to distribution of the second-order quadrupole shift, it remains sharp up to 7.2 GPa for *H* || *c*. The vertical dashed line represents the unshifted resonance position $f_{\text{res}}\gamma^{-1}$ (=6.63 T). (b) The spectra in the AF state for *H* || *c* (red) and *H* ⊥ *c* (blue). The gray arrows indicate the splitting (*H* || *c*) or the shift (*H* ⊥ *c*) induced by the hyperfine fields ± Δ along the *c* axis, transferred from the stripe-type AF Fe moments [illustrated at the right-top corner in (a)]. There are four satellite lines for *H* ⊥ *c*, indicating the twinned orthorhombic structure with asymmetric electric field gradients.

α direction. In the AF state the spectra for $H \parallel c$ split symmetrically into two sets of three lines. However, the central line ($m = 1/2$) for $H \perp c$ does not split, indicating that the hyperfine fields are parallel to the c -axis, $H_{\text{hf}} = (0, 0, \pm\Delta)$. This is compatible with the commensurate stripe AF structure with $\mathbf{q} = [101]$ and the AF moments parallel to the a axis as previously reported [6,14]. Our results prove that the ground state below 4.2 GPa has the stripe-type AF order with the orthorhombic structure.

The AF transition temperature T_N can be determined from the vanishing of the PM spectral intensity [Fig. 2(a)]. The hysteresis provides clear evidence for a first-order transition. Below 4.2 GPa, no fraction of the PM state remains at low T . Figure 2(b) shows T dependence of the nuclear spin-lattice relaxation rate T_1^{-1} divided by T . $(T_1 T)^{-1}$ shows an upturn as T approaches T_N below 4.2 GPa, indicating development of AF spin fluctuations

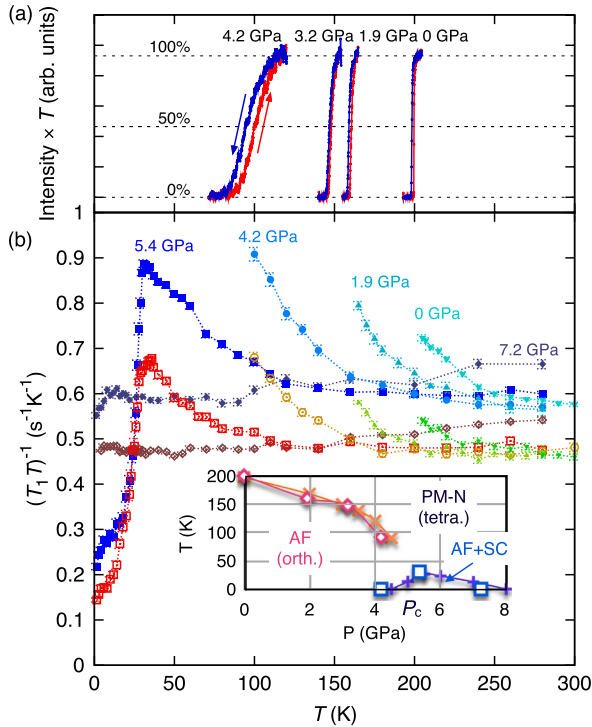


FIG. 2 (color online). (a) The AF transition detected by tracking the peak intensity of the PM central line for $H \parallel c$. The rates for the T sweep were kept slower than 0.05, 0.1, 0.3 K/min. for 1.9, 3.2, 4.2 GPa, respectively. Sharp transition with hysteresis demonstrates good homogeneity of the sample and the first-order AF transition. (b) $(T_1 T)^{-1}$ in the PM state for $H \perp c$ (the plots in dark blue to sky blue with higher values) and for $H \parallel c$ (the lower plots in brown to green). The inset shows the P - T phase diagram. T_N is determined from the 50% recovery of the PM intensity on warming in (a) (open diamonds). The bulk SC transition (open squares) is detected in our NMR experiment only at 5.4 GPa. T_c is determined from the peak in $(T_1 T)^{-1}$ at 11 T for $H \perp c$. The SC transition is absent below 4.2 and at 7.2 GPa. Crosses represent the data reported based on the resistivity (for AF) and the ac susceptibility (for SC) measurements [11].

in the PM state even though the transition is first-order. At 5.4 GPa, an increase of $(T_1 T)^{-1}$ is also observed above 30 K, followed by a sudden decrease at lower T . As we discuss later, the PM spectrum does not vanish at low T at 5.4 GPa and there is sufficient evidence for a bulk SC state. The reduction of $(T_1 T)^{-1}$ is then a consequence of opening of the energy gap in the SC state. When P is increased to 7.2 GPa, $(T_1 T)^{-1}$ is nearly independent of T , exhibiting neither an SC transition nor development of AF fluctuations.

Let us examine the microscopic features of the SC state at 5.4 GPa. Figure 3 shows the NMR spectra obtained by sweeping frequency at fixed fields [15]. The spectra immediately above the SC transition temperature T_c show identical features to those at 35 K [Fig. 1(a)], and hence belong to the PM and normal (N) state. The central line for $H \parallel c$ broadens suddenly below T_c [see the insets and Fig. 3(b)] due to field distribution in the SC mixed state. At 4.2 K, the spectra clearly show coexistence of the tetragonal PM-SC and the orthorhombic AF domains with comparable volume fractions as indicated in Figs. 3(a) and 3(c). The broad asymmetric central line for $H \perp c$ at 26 K [Fig. 3(c)] indicates that the AF domains appear immediately below T_c . Thus only one phase transition from the N-PM state to the SC/AF coexisting state occurs over the entire sample. This would not be possible if the coexistence were due to inhomogeneity. Instead, the results strongly suggest formation of a self-organized SC/AF hybrid structure.

The T dependence of $(T_1 T)^{-1}$ and the Knight shifts were measured at 5.4 GPa [Figs. 4(a) and 4(b)]. Both exhibit sudden decrease due to opening of the SC gap with spin-singlet pairing below $T_c = 27$ –30 K, depending slightly on the field values. The values of T_c agree well with the onset of the diamagnetic response [Fig. 4(c)]. These results provide definitive evidence for the bulk SC state. What is anomalous though is that $(T_1 T)^{-1}$ approaches a finite value towards 0 K, indicating a finite density of state (DOS), i.e., gapless superconductivity. Moreover, the SC and AF domains show nearly the same value of $(T_1 T)^{-1}$ at low T . To demonstrate good electronic homogeneity, the recovery curves in the relaxation measurements are shown in Figs. 4(d)–4(f) at several T . All curves are fit extremely well by assuming a single value of T_1^{-1} . Since even minor disorder often causes significant distribution in T_1^{-1} , this is a stringent proof for good homogeneity. Therefore, the coexistence of SC/AF domains and the residual DOS in the SC domains are intrinsic and free from material inhomogeneity. The origin of the residual DOS should be one of the following: (i) pair breaking due to disorder or magnetic field, (ii) existence of gapless Fermi surfaces not involved in the SC pairing, or (iii) proximity effect from nearby AF domains. We can exclude the case (i) based on the nearly field-independent and uniform behavior of $(T_1 T)^{-1}$. Since the gapless behavior persists down to 1.5 K, orders of magnitude smaller than T_c , the case (ii)

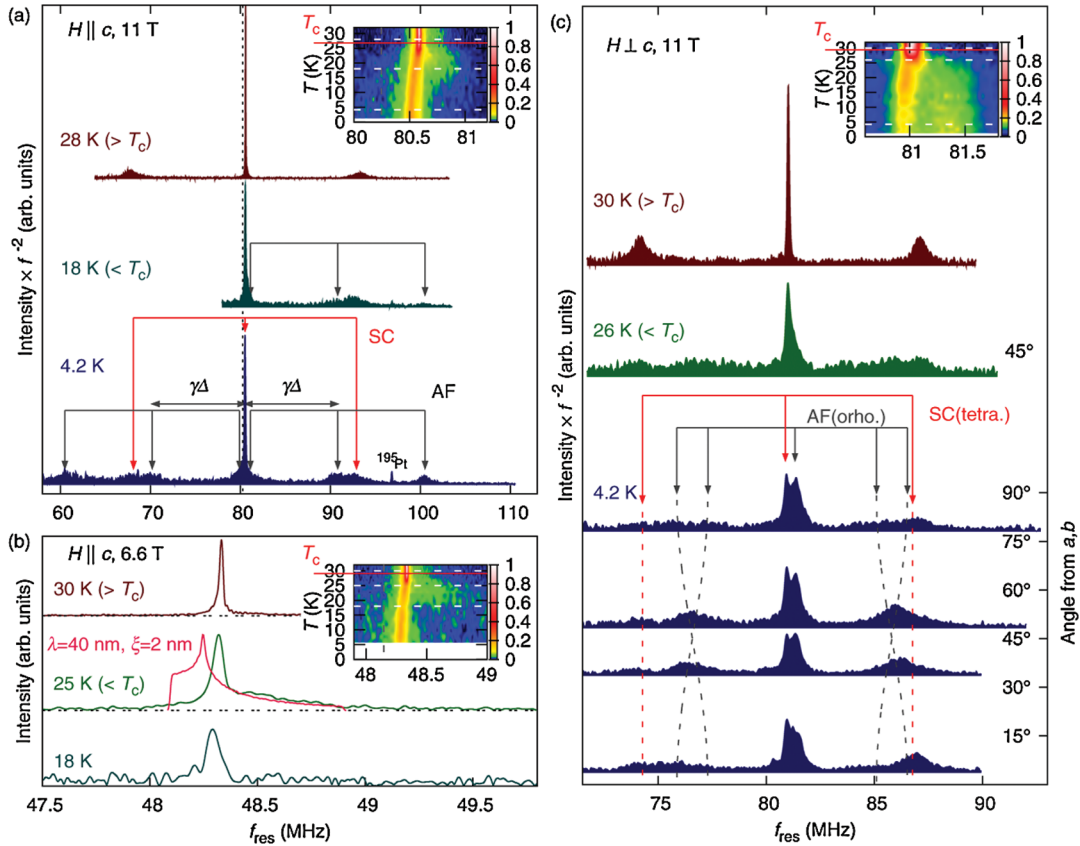


FIG. 3 (color). ^{75}As -NMR spectra at 5.4 GPa showing the coexistence of the AF and SC states. The insets show the color plots indicating the T dependence of the spectral intensity distribution near the central line. The white dashed lines indicate the T values of the spectra in the main panels. (a) The NMR spectra for $H \parallel c$ at 11 T measured at 28 K (above T_c), 18 K (below T_c), and 4.2 K. At 4.2 K, the spectrum shows contributions both from the commensurate stripe-type AF domains (gray arrows) and from the PM-SC domains (red arrows). (b) The PM (SC or normal) central lines for $H \parallel c$ at 6.6 T. Anomalous line shape with asymmetric broad tail is observed for $18 \text{ K} < T < T_c$ (see the inset). Standard models of vortex lattices are unable to fit the spectrum at 25 K even if an extremely short penetration depth λ is assumed. An example, is shown by the red line calculated with the modified London model for a rectangular vortex lattice [19,22,23]. (c) The spectra for $H \perp c$ at 11 T. At 4.2 K, the satellite lines from the AF domains split into two sets. The azimuth angle dependence of the satellite positions in the ab -plane are reproduced by the asymmetry parameter $|(\nu_a - \nu_b)/\nu_c| = 0.15$ as shown by the dashed lines. This proves the twinned orthorhombic structure of the AF domains. The broadened spectrum at 26 K from the AF domains indicates modulation of AF moments and the structure, most likely an incommensurate spin-density-wave type.

alone is also unlikely. Nevertheless, proximity effects from the AF domains (case iii) can squeeze small gaps on parts of the Fermi surfaces. Note that the size of SC domains must be sufficiently small in order for proximity to be effective. This suggests spontaneous formation of nano-scale periodic structure of alternating SC and AF domains.

We now add the SC phase boundary to the P - T phase diagram in the inset of Fig. 2(b). The SC/AF hybrid state appears only in a very narrow P region over 5 GPa. It is reported that improved hydrostaticity results in higher critical pressure P_c for the appearance of the SC state [16]. Our value $P_c \sim 5$ GPa is higher than the previous results, indicating good hydrostaticity of argon medium. The narrow P range of the SC state is in marked contrast to the stable pure SC state obtained by chemical doping [7,8,17,18], and points to a rather fragile nature of the SC/AF hybrid state. Note that the equal numbers of elec-

trons and holes are preserved under pressure but not by doping.

Next, we focus on the T dependence of the spectra at 5.4 GPa immediately below T_c . We first discuss the spectra from the AF domains. For $H \parallel c$, the spectral intensity from the commensurate AF domains is reduced with increasing T and only weakly visible at 18 K [Fig. 3(a)]. On the other hand, for $H \perp c$, the AF spectra do not lose intensity but broaden near T_c . The asymmetric broadening of the central line and the much wider satellites of the spectrum at 26 K [Fig. 3(c)] indicate incommensurate modulation in both the AF moments and the structure. Since even the second-order effect of H_{hf} for $H \perp c$ causes substantial broadening, the first-order effects should easily wipe out the AF spectra for $H \parallel c$, explaining the loss of intensity. Our results then suggest a crossover at $T^* \sim 18$ K from the low- T stripe AF state with a uniform mag-

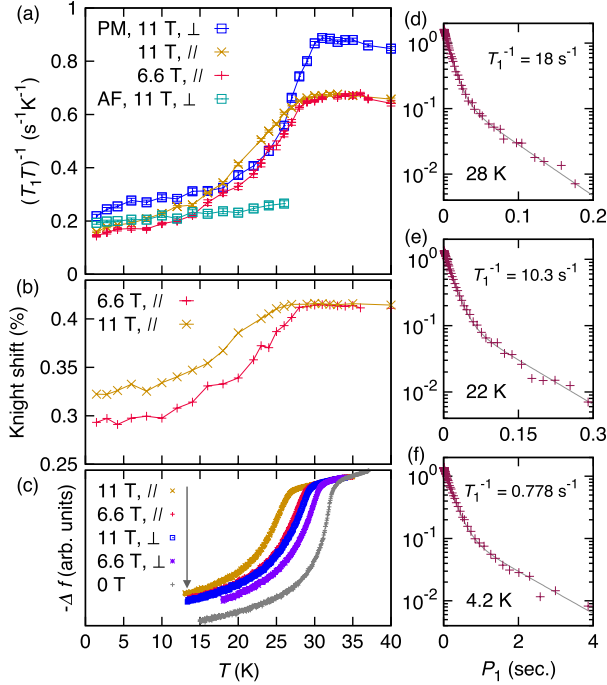


FIG. 4 (color online). Evidence for bulk SC state at 5.4 GPa. (a) The T dependence of $(T_1T)^{-1}$ in the PM state for $H \perp c$ at 11 T (blue) and for $H \parallel c$ at 11 T (orange) and at 6.6 T (red). The blue and the red data are identical to those shown in Fig. 2(b). Opening of the SC gap causes sudden decrease of $(T_1T)^{-1}$ below T_c . Also shown are $(T_1T)^{-1}$ data in the AF state for $H \perp c$ at 11 T (sky blue). All measurements were made on the central line, whose positions are shown by the arrows in Fig. 3. (b) The T dependence of the Knight shift for $H \parallel c$ at 6.6 and 11 T. The reduction below T_c indicates the spin-singlet pairing in the SC state. (c) The ac susceptibility measured by the self resonance method using the NMR coil. The change of the resonating frequency $-\Delta f$ represents the Meissner shielding. (d)–(f) Typical recovery curves of the nuclear magnetization during the T_1 measurement at 28 K (immediately above T_c), 22 K, and 4.2 K (below T_c) for $H \parallel c$ at 11 T. Each curve is fit very well to the formula for spin 3/2 nuclei, $\{\exp(-t/T_1) + 9 \exp(-6t/T_1)\}/10$, with a single value of T_1 , supporting uniform relaxation process.

nitude of moments to the high- T modulated (incommensurate) structure.

In the same T region ($T^* < T < T_c$), we observed anomalous spectral shape as shown in Fig. 3(b). The central line at 25 K for $H \parallel c$ consists of a moderately broadened line on top of a much broader tail. While the former persists to low T , the latter disappears below T^* . Since similar values of T_1^{-1} are obtained on and off the main peak, they both belong to the SC-PM domain. Note that T_1^{-1} for the AF domain is smaller by a factor of 3 at 25 K [Fig. 4(a)]. The width of the broad tail decreases slightly with increasing field, indicating that the origin is related to the SC diamagnetic current. Nevertheless, the entire line shape cannot be explained by standard vortex lattices with any choice of parameters (see the red line).

The puzzling line shape above T^* indicates anomalous modulation of the SC diamagnetic current with a much shorter length scale than the penetration depth, where modulation of the AF moments also appears.

Coexistence of AF and SC states has been observed in some heavy fermion compounds. For example, CeRhIn_5 under pressure shows microscopic coexistence of the AF and SC orders, which are spatially indistinguishable [19,20]. In CeIn_3 the AF and SC orders occur in different spatial region at different transition temperatures [19,21]. The case of SrFe_2As_2 differs from any of examples known to date in that the SC and AF orders are spatially distinguished but occur simultaneously forming a spontaneous SC/AF hybrid structure.

We thank M. Ogata, Y. Yanase, K. Ishida, M. Yoshida, K. Matsubayashi, and A. Yamada for their help and discussions. This work supported by the Grant-in-Aid for Scientific Research (B) (No. 21340092 and No. 21340093) from JSPS and by the GCOE program from MEXT. K. K. is supported by the JSPS.

*kitag@issp.u-tokyo.ac.jp

†Present address: Department of Physics, University of Virginia, Charlottesville, VA 22904, USA.

- [1] Y. J. Uemura, *Nature Mater.* **8**, 253 (2009).
- [2] K. Ishida *et al.*, *J. Phys. Soc. Jpn.* **78**, 062001 (2009).
- [3] J. T. Park *et al.*, *Phys. Rev. Lett.* **102**, 117006 (2009).
- [4] D. K. Pratt *et al.*, *Phys. Rev. Lett.* **103**, 087001 (2009).
- [5] K. Kaneko *et al.*, *Phys. Rev. B* **78**, 212502 (2008).
- [6] K. Kitagawa *et al.*, *J. Phys. Soc. Jpn.* **78**, 063706 (2009).
- [7] K. Sasmal *et al.*, *Phys. Rev. Lett.* **101**, 107007 (2008).
- [8] A. Leithe-Jasper *et al.*, *Phys. Rev. Lett.* **101**, 207004 (2008).
- [9] P. L. Alireza *et al.*, *J. Phys. Condens. Matter* **21**, 012208 (2009).
- [10] H. Kotegawa *et al.*, *J. Phys. Soc. Jpn.* **78**, 013709 (2009).
- [11] K. Matsubayashi *et al.*, *J. Phys. Soc. Jpn.* **78**, 073706 (2009).
- [12] K. Kitagawa *et al.*, arXiv:0910.1767v2 [*J. Phys. Soc. Jpn.* (to be published)].
- [13] N. Tateiwa and Y. Haga, *Rev. Sci. Instrum.* **80**, 123901 (2009).
- [14] K. Kitagawa *et al.*, *J. Phys. Soc. Jpn.* **77**, 114709 (2008).
- [15] Each Fourier spectrum of an echo is summed while the frequency is being swept [Fourier-step-summing (FSS)]. To take the spectrum over a very wide frequency range, we superpose the FSS power spectra by shifting the center frequency by 1 MHz and readjusting the electric circuit and transmitting power.
- [16] H. Kotegawa *et al.*, *J. Phys. Soc. Jpn.* **78**, 083702 (2009).
- [17] Y. Kamihara *et al.*, *J. Am. Chem. Soc.* **130**, 3296 (2008).
- [18] M. Rotter *et al.*, *Phys. Rev. Lett.* **101**, 107006 (2008).
- [19] N. J. Curro, *Rep. Prog. Phys.* **72**, 026502 (2009).
- [20] S. Kawasaki *et al.*, *Phys. Rev. Lett.* **91**, 137001 (2003).
- [21] S. Kawasaki *et al.*, *J. Phys. Soc. Jpn.* **73**, 1647 (2004).
- [22] A. Yaouanc *et al.*, *Phys. Rev. B* **55**, 11 107 (1997).
- [23] Y. Nakai *et al.*, *J. Phys. Soc. Jpn.* **77**, 333 (2008).